Available online at www.sciencedirect.com

ScienceDirect

Procedia CIRP 46 (2016) 603 – 606

www.elsevier.com/locate/procedia

7th HPC 2016 – CIRP Conference on High Performance Cutting

# Modelling and simulation of grinding processes with mounted points: Part II of II - Fast modelling method for workpiece surface prediction

E. Uhlmann[a,b], S. Koprowski[a,*], W. L. Weingaertner[c], D. A. Rolon[a]

[a] *Fraunhofer – Institute for Production Systems and Design Technology (IPK), Pascalstr. 8-9, 10587 Berlin, Germany*
[b] *Technical University Berlin – Institute for Machine Tools and Factory Management (IWF), Pascalstr. 8-9, 10587 Berlin, Germany*
[c] *Department of Mechanical Engineering, Federal University of Santa Catarina, 88040-900 Florianópolis, SC, Brazil*

[*] Corresponding author. Tel.: +49 (0)30 / 39 006 148; fax: +49 (0)30 / 39 110 37. *E-mail address:* stefan.koprowski@ipk-projekt.fraunhofer.de

**Abstract**

Due to the importance of high surface quality of machined parts, considering its functional requirements, it is important to select a proper set of grinding parameters. Experimental trials are material, energy and time consuming. Therefore it is relevant for the industry to use a roughness model capable of simulating different grinding kinematics with different sets of parameters. This paper presents a fast and reliable method, for the NC-grinding process with abrasive mounted points, to reach this demand. In order to achieve this, numerical and empirical experiments were conducted proving the feasibility of the model for conventional, oscillating and tilt surface grinding.

Peer-review under responsibility of the International Scientific Committee of 7th HPC 2016 in the person of the Conference Chair Prof. Matthias Putz
*Keywords:* Grinding, Simulation, Kinematic.

## 1. Introduction

Grinding processes consist of a large amount of abrasive grains, bounded with a specific material, which interacts with a workpiece in order to remove material to achieve project specifications [1]. Due to the complex interaction between system and process parameters with the results, it is difficult to model a reliable simulation to be used for industrial applications [2]. However, in the past decades, the demand of reliable models and simulations has grown due to the development of new technologies and the need of more accuracy of machined parts. Consequently, to achieve more reliable results, it demands a better understanding of the grinding process [3].

The development of modern computers allowed an introduction of the first modelling systems for different grinding processes. For example, simulations to anticipate various aspects of wheel wear behavior [4], grinding force and power [5], and tool-workpiece interaction [6]. To predict the grinding process behavior there are several process model methods (fundamental analytical and finite element), empirical process models (regression and artificial neural net models) and heuristic process models (rule based models) [7].

Recent simulation studies can be applied for new kinematics, such as the ones proposed by Uhlmann [8] and parameter optimization for grinding with mounted points [9]. Among these kinematics, three can be pointed out. These are conventional surface grinding (CSG), oscillation surface grinding (OSG) and tilt surface grinding (TSG). To model different strategies and process parameters, main steps should be considered, such as the characterization of the grinding tool, geometry and its interaction with the workpiece during contact as well with the material removal.

With a reliable model to describe the grinding tool presented on the paper part I, this paper, part II, aims to develop a fast method to predict the structure of ground surfaces for different process parameters (e.g. feed rate $v_f$, worktool rotation $n$, structure angle $\alpha_s$, oscillation frequency $f_s$ and amplitude $A_s$) and different grinding kinematics (e.g. CSG, OSG and TSG).

## 2. Grinding kinematics

The structure angle $\alpha_s$ was introduced as one of the most significant parameters for grinding with abrasive mounted points [8,9]. This parameter results from the orientation of the scratches, which is related to the cutting speed $v_c$, and the repetition of it along the grinding tool path due to the feed rate $v_f$. Thus, the structure angle is a direct resultant of the kinematics during the grinding process.


Peer-review under responsibility of the International Scientific Committee of 7th HPC 2016 in the person of the Conference Chair Prof. Matthias Putz
doi:10.1016/j.procir.2016.03.202

For instance, in CSG, the orientation of the scratches have the same direction of the grinding tool path, which results into a structure angle $\alpha_s$ of 0° (fig. 1a). In OSG, the average oscillation velocity $\overline{v_{os}}$ is a consequence of the additional axial displacement $\overline{v_h}$ of the grinding tool along with its radial velocity $v_r$. Due to this oscillation displacement, the outcome scratches are aligned into a waveform along the workpiece surface (fig. 1b). This waveform posses a defined amplitude $A_s$ and a frequency $f_s$, which means a variation of the structure angle along the workpiece surface. Therefore, a way to characterize the OSG kinematic is by the average structure angle $\overline{\alpha_s}$. When the outcome scratches possess a fixed angle in relation to the feed rate $v_f$, the kinematic is called TSG (fig. 1c). This kinematic results in a uniform structure angle $\alpha_s$ along the workpiece surface.

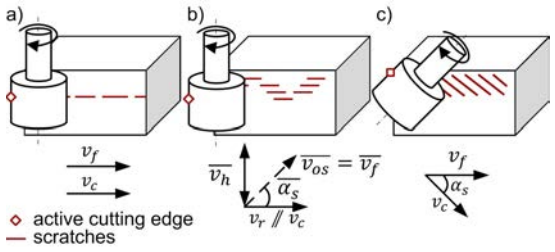


Figure 1. Kinematic scheme of (a) CSG, (b) OSG and (c) TSG. Adapted from Uhlmann [8].

## 3. Experimental Setup

### 3.1. Methodology

The steps presented in this chapter, aims to show the methodology, shown in fig. 2, applied to validate the geometrical simulation.

The experiments (#1, #2 and #3) were proposed to acquire different surface structures for CSG, OSG and TSG kinematics. Then, to compare them with the simulation results (S1, S2 and S3) in order to validate the geometrical simulation by verifying the changes of the structure along the simulated surface and the experimental ground workpieces.

For presenting a potential application of the simulation method, different simulation trials were conducted, in which

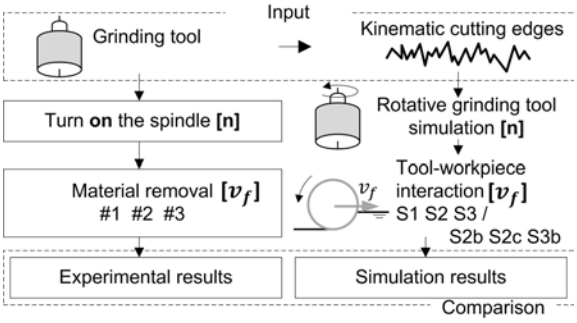


Figure 2. Scheme of the methodology applied.

different process parameters were used. For S2b, the oscillation amplitude $As$ of the case #2 was set to 1 mm and for S2c the frequency $f_s$ was set to 0.4 Hz. For S3b, the structure angle $\alpha_s$ of the case #3 was reduced to 15°. For the simulations, a commercial laptop was used.

### 3.2. Experimental Process

Experimental tests were conducted by using a 5-axis-grinding machine tool RXP600DSH UHP from Röeders GmbH, Soltau, Germany, using an electroplated diamond mounted point tool. In table 1 are listed the grinding tool and workpiece characteristics and conditioning parameters used for the investigations. The grinding parameters are listed in tab. 2.

Table 1. Grinding tool and workpiece characteristics and conditioning parameters.

| | |
|---|---|
| *Grinding tool* | |
| Shape (Diameter, Lenght) | Cilindrical (8 mm, 8 mm) |
| Grain type, concentration | D 126, C100 |
| Bond type | Electroplated |
| *Conditioning parameters* | |
| Tool | Winter No2, EKW 180 I9 V900 |
| Sharpening tool feed rate $v_{fSb}$ | 200 mm/min |
| Sharpening tool feed $a_{Sb}$ | 2 mm |
| Sharpening tool height $h_{Sb}$ | 6 mm |
| *Workpiece* | |
| Material | Graphite |
| Average Particle Size | <1 $\mu$m |
| Hardness | 83 shore |
| Dimensions | 50 mm x 100 mm x 20 mm |

Regarding the workpiece, graphite pieces, with particle size lower than 1 $\mu$m, were selected due to its low hardness thus diminishing the grinding tool wear and providing a high reliability of the process.

Table 2. Grinding parameters for the experimental trials.

| Case | #1 | #2 | #3 |
|---|---|---|---|
| Kinematic | CSG | OSG | TSG |
| Periferal velocity $v_s$ [m/s] | 20 | 20 | 20 |
| Feed rate $v_f$ [mm/min] | 50 | 50 | 50 |
| Depth of cut $a_e$ [mm] | 0.150 | 0.150 | 0.150 |
| Oscillation | no | yes | no |
| Amplitude $A_s$ [mm] | - | 0.5 | - |
| Frequency $f_s$ [Hz] | - | 0.2 | - |
| Tilt | no | no | yes |
| Structure angle $\alpha_s$ [°] | - | - | 30 |

## 4. Numerical simulation steps

The simulation steps are described in this section. The representation of these steps are presentented in in fig. 3 using OSG kinematic.

### 4.1. Input

For the modelling of the grinding process with abrasive mounted points, it is essential to have a knowledge about the

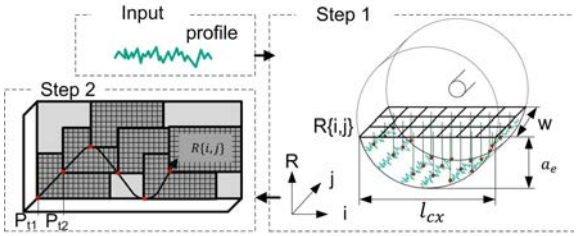


Figure 3. Steps of the geometrical simulation.

grinding tool topography. Therefore, as described in the paper part I, a profile that represents the kinematic cutting edges of the grinding tool was used as an input. The profile can be acquired with a scratch test.

### 4.2. Step 1: Rotary grinding tool

The first step of the simulation describes the rotary grinding tool as a matrix R{$i$, $j$}. In this step, the kinematic cutting edges profile is positioned along the $j$ axis and replicated along the $i$ axis, in which the grinding tool matrix R{$i$, $j$} varies according to the grinding tool diameter $D$ (fig. 3 Step 1), then modelling the rotary grinding tool R{$i$, $j$}. This step 1, resembles the act of turning on the spindle of a grinding machine (fig. 2).

Regarding the lateral resolution of the rotary grinding tool matrix R{$i$, $j$}, its value relies on the kinematic cutting edge profile used as input. The maximum length of the columns $j$ represents the grinding tool width $w$ and the length $i$ is calculated based on the contact length $l_{cx}$.

### 4.3. Step 2: Tool-workpiece interaction

On Step 2, the relative movement between grinding tool and workpiece is added, simulating the material removal with a defined depth of cut $a_e$. The rotary grinding tool matrix R{$i$, $j$}, in this Step 2, is positioned along the matrix which represents the workpiece z{$x, y$} for each rotation of the grinding tool.

The rotation of the grinding tool is constant along the simulated process, so the time of each rotation $t_s$ is calculated according to Eq. 1, defining the temporal discretisation of the present simulation. The displacement of the rotary grinding tool R{$i$, $j$} over the workpiece z{$x, y$} are obteined according the equations 2 and 3.

$$t_s = \frac{60}{n} \tag{1}$$

$$x(t) = v_f \cdot t \tag{2}$$

$$y(t) = A_s \cdot sin(t \cdot f_s \cdot 2\pi) \tag{3}$$

The variation of the displacement of the grinding tool along the $y$ axis only occur during the OSG. For CSG and TSG, the values of frequency ($f_s$) and amplitude ($A_s$) will be zero, hence nullifying the term $y$ and having the displacement only in $x$ axis. For TSG, as the the structure angle $\alpha_s$ must be considered, the rotary grinding tool matrix R{$i$, $j$} must be tilted in relation to the $z$ axis. For adding this tilt angle to the rotary grinding tool matrix R{$i$, $j$}, the Eq. 4 was used.

$$\begin{bmatrix} R' \\ i' \\ j' \end{bmatrix} = \begin{bmatrix} 1 & 0 & 0 \\ 0 & cos(\alpha_s) & -sin(\alpha_s) \\ 0 & sin(\alpha_s) & cos(\alpha_s) \end{bmatrix} \cdot \begin{bmatrix} R \\ i \\ j \end{bmatrix} \tag{4}$$

## 5. Results

Fig.4 shows the output of each of the steps for OSG simulation, which its input is the kinematic cutting edges profile acquired with a scratch test, as presented in the paper part I. Step 1 shows the resultant rotaring grinding tool and Step 2 shows the structure of a ground surface.

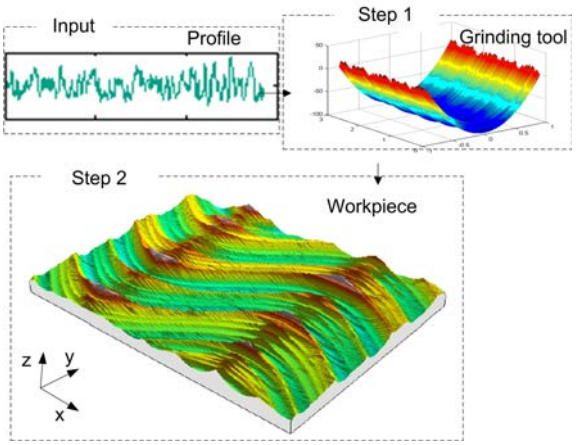


Figure 4. Steps of the geometrical simulation.

Experimental trials were carried out to validate the simulations. The measured surfaces are shown in fig. 5a for the cases #1, #2 and #3. Concerning the simulation results, these are presented for qualitative comparison in fig. 5b (S1, S2 and S3). Both, simulation and experiments results, shows an improvement of the surface for OSG and TSG when compared to the CSG, according to the proposed by Uhlmann. [8,9]. Not only in a qualitative way, the surface structure improvements are also noticed with the surface parameters according to ISO 25178, presented in tab. 3.

Table 3. Surface parameters according ISO 25178.

| Case | #1 | S1 | #2 | S2 | S2b | S2c | #3 | S3 | S3b |
|---|---|---|---|---|---|---|---|---|---|
| Sq | 5.23 | 5.03 | 3.80 | 3.57 | 2.73 | 2.83 | 3.15 | 2.79 | 3.74 |
| Sz | 33.6 | 21.4 | 29.7 | 22.0 | 17.7 | 20.2 | 25.3 | 12.1 | 18.1 |
| Sa | 4.35 | 4.30 | 3.06 | 2.93 | 2.16 | 2.20 | 2.56 | 2.37 | 3.09 |
| Sk | 12.7 | 11.5 | 6.93 | 5.93 | 4.34 | 4.47 | 5.96 | 4.21 | 6.06 |
| Spk | 3.13 | 2.35 | 3.55 | 3.70 | 2.76 | 2.68 | 2.46 | 2.87 | 4.82 |
| Svk | 2.73 | 2.06 | 2.17 | 1.89 | 1.05 | 1.42 | 1.90 | 0.98 | 2.06 |

* values in $\mu$m.

Both, S2b and S2c, using OSG kinematic show a reduction of the surface parameters compared to the S2 as shown in tab. 3. However, for S3b, the structure angle of 15° led to a higher surface parameters than S3.

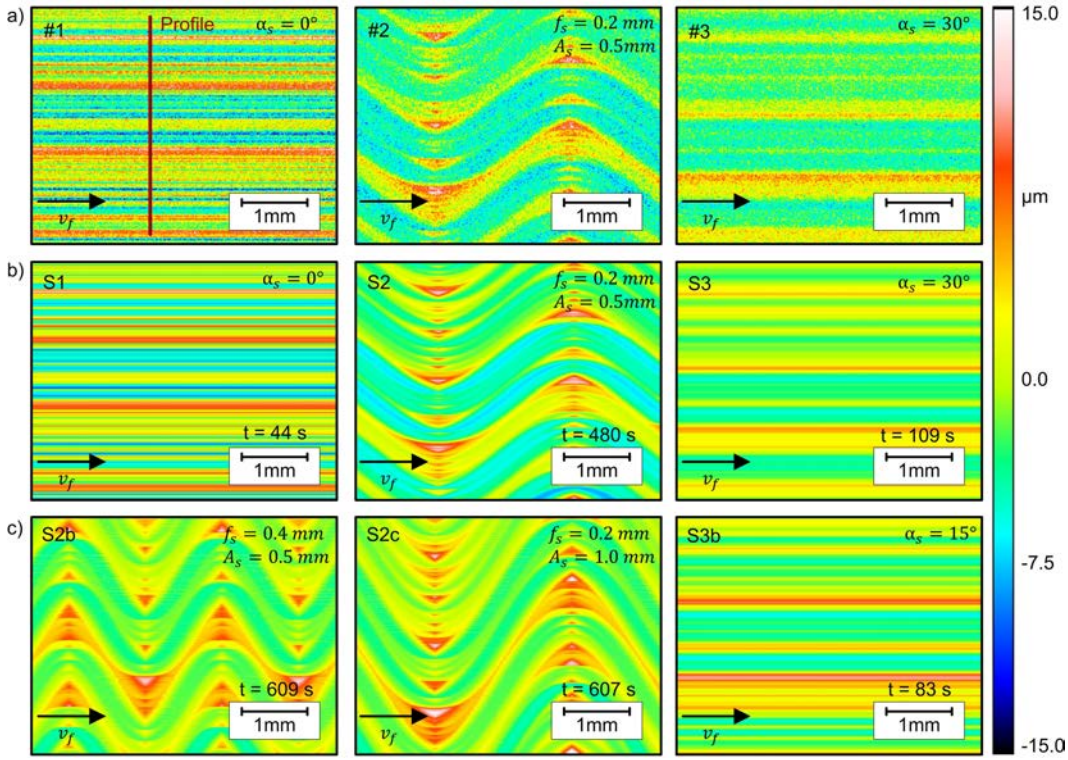


Figure 5. Top view of the measured surfaces #1, #2 and #3 (a), of the simulation results S1, S2 and S3 (b) and the simulation results S2b, S2c and S3b (c).

Knowing that the simulation outputs are results from a certain amount of computer processing time, each simulation is presented in fig. 5 with their corresponding processing time.

## 6. Summary and conclusions

In accordance with the experimental results, the numerical simulation followed the same tendency for the different kinematics. This can be noticed in a qualitative analysis and based on the analysis of the surface parameters. Due to these results, the simulation proved to be a reliable tool to predict the surface structure for CSG, OSG and TSG kinematics.

In order to study process optimization, an improvement regarding the different parameters applied in S2b and S2c comparing with S2 was shown in fig. 5(c) and tab. 3. But for S3b, the new parameters shown a worse surface characteristics compared to S3. Using this simulation method, parameters variation could be analyzed and optimized in a short period of time.

For studying the different kinematics, the grinding tool was considerate perfectly rigid. Moreover, possible deflection of the abrasive grains and grinding tool wear was disregarded. Data considering the minimum depth of cut can be included in this model in future studies, along with material removal conditions, such as ductile and fragile behavior along with tool deflection, grinding force and grinding tool wear.

## Acknowledgements

We would like to acknowledge the scholarship given by CAPES Foundation to the corresponding author. Supported by the Ministry of Education, Brasilia, Brazil.

## References

[1] Klocke F, König W. Fertigungsverfahren 2; 4th Ed. Springer; 2013. p. 463, 2005.
[2] Stepien P. A probabilistic model of the grinding process. Applied Mathematical Modelling, 33, p. 3863-3884; 2009.
[3] Doman DA, Warkentin A, Bauer R. A survey of recent grinding wheel topography models International Journal of Machine Tools and Manufacture, 46, p. 343-352; 2006.
[4] Chen X, Rowe WB, Mills B, Allanson DR. Analysis and simulation of the grinding process. Part IV: Effects of wheel wear. International Journal of Machine Tools Manufacturing, p. 41-49; 1998.
[5] Hecker RL, Liang SY, Wu XJ, Xia PJ, Jin DGW. Grinding force and power modeling based on chip thickness analysis. International Journal of Advanced Manufacturing Technologies, p. 449-459; 2003.
[6] Nguyen TA, Butler DL. Simulation of surface grinding process, part 2: interaction of the abrasive grain with the workpiece. International Journal Of Machine Tools and Manufacture, p. 1329-1336; 2005.
[7] Chuang T, Jahanmir S, Tang HC. Finite element simulation of straight plunge grinding for advanced ceramics. Journal Of The European Ceramic Society, vol. 23, p. 1723-1733; 2002.
[8] Uhlmann E, Borsoi Klein T, Koprowski S. Tilt angle effects in surface grinding with mounted points. Production Engineering Research and Development, vol. 8, p. 431–442; 2014.
[9] Uhlmann E, Borsoi Klein T, Hochschild L, Bäcker C. Influence of structuring by abrasive machining on the tribological properties of workpiece surfaces. In: Procedia engineering, 1st CIRP conference on surface integrity (CSI), vol. 19, p. 363–370; 2011.